JOURNAL OF MATERIALS SCIENCE 31 (1996) 4899–4906

Microstructure, chemical reaction and mechanical properties of TiC/Si_3N_4 and TiN-coated TiC/Si_3N_4 composites

JOW-LAY HUANG, MING-TUNG LEE, HORNG-HWA LU
Department of Material Science and Engineering, National Cheng-Kung University, Tainan, Taiwan 701

DING-FWU LII
Department of Electrical Engineering, Chinese Naval Academy, Kaohsiung, Taiwan 813

Silicon nitride containing various compositions of as-received TiC and TiN-coated TiC, were hot pressed at 1800 °C for 1 h in a nitrogen atmosphere. In TiN-coated TiC/Si_3N_4 composites, TiC reacted first with the TiN coating to form a titanium carbonitride interlayer at 1450 °C, which essentially reduced further reactions between TiC and Si_3N_4 and enhanced densification. TiN-coated TiC/Si_3N_4 composites exhibited better densification, hardness, flexural strength and fracture toughness than those of as-received TiC/Si_3N_4. The toughening mechanisms for as-received TiC/Si_3N_4 and TiN-coated TiC/Si_3N_4 composite were attributed to crack deflection, load transfer and crack impedence by the compressive thermal residual stress.

1. Introduction

Silicon-based non-oxide ceramics have received much attention on account of their two potential applications: engine components and cutting tools. Both of these usages require good mechanical properties, chemical stability and, especially, reliability at elevated temperatures. Ceramic-reinforced silicon nitride is known to be possibly one of the most utilized materials for high-temperature structural applications.

The most notable mechanical properties of titanium carbide at high temperatures are the high melting point, extreme hardness and strength, good chemical stability and adequate erosion and corrosion resistance. Recently, silicon nitride toughened with titanium carbide has been developed as a new class of structural ceramic materials [1–4]. The toughness of silicon nitride has been reported to be enhanced more than 50% by the incorporation of TiC particulates [1]. Another advantage of incorporating TiC into Si_3N_4 is that the conductivity of Si_3N_4 can be substantially increased which, consequently, makes electric discharge machining (EDM) possible [2]. One drawback with the TiC/Si_3N_4 was, however, that the chemical reactions between TiC and Si_3N_4 could degrade somewhat the hardness, fracture toughness, and high-temperature strength [3, 5, 6].

It has been reported [7, 8] the TiN was quite chemically stable in Si_3N_4 up to a temperature of 1800 °C. The effectiveness of coating TiN on ceramic powders for successfully improving the properties of sintered bodies, has also been reported [9, 10]. In the present study, TiN was selected for coating on to the TiC particulates via a chemical vapour deposition (CVD) method before adding into the Si_3N_4 matrix. The microstructure and phase development in both as-received TiC/Si_3N_4 and TiN-coated TiC/Si_3N_4 composites were investigated and the results were compared with calculations derived from thermodynamic considerations. Some mechanical properties were evaluated and correlated with the developed microstructure.

2. Experimental procedure

2.1. Powder preparation

Silicon nitride powder (LC12, H.C. Stark, Goslar, FRG), size 0.6 μm, was mixed with yttria (5603, Molycorp, White Plains, NY, 1.8 μm) and alumina (16 SG, Alcoa, Bauxite, AK, 0.5 μm) in a polyurethane bottle with high-purity alumina balls and ethanol for 22 h. The ratio of ball to charge to vehicle was 6:1:5 by mass.

Titanium carbide (T-1251, Cerac, Milwaukee, Wi, USA) powders, size 10 μm, were uniformly placed inside an alumina crucible, set in conventional CVD reaction furnace. A schematic drawing of the CVD apparatus is shown in Fig. 1. The reaction gases used were $TiCl_4$ (8 $cm^3 min^{-1}$), nitrogen (270 $cm^3 min^{-1}$) and hydrogen (290 $cm^3 min^{-1}$). The TiN was deposited at 1050 °C under 1 atm pressure for 1.5 h. The TiN-coated TiC (CVD-TiC) powders were then ground and screened through a 325 mesh screen.

Both TiN-coated TiC and as-received TiC powders (10%, 20%, 30% total volume) were separately

0022–2461

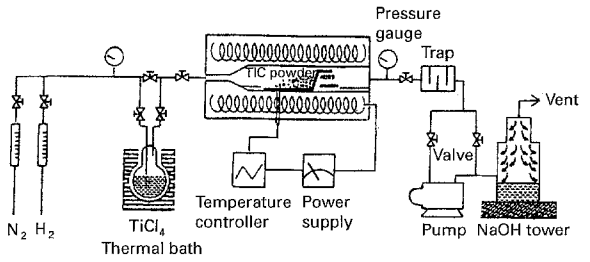

Figure 1 Schematic diagram of the experimental apparatus for CVD-TiN.

dispersed by means of an ultrasonic probe in ethanol, added to the Si_3N_4 slurry and milled for 2 h. The slurry was then ultrasonically dispersed for an additional 3 min and dried in a rotating vacuum condenser. Dried agglomerates were ground with an alumina mortar and pestle, and screened through a 100 mesh screen to pulverize the aggregates.

2.2. Analysis of TiN-coated TiC powders

The phases of CVD-processed TiC-powders were determined by X-ray diffractometry (Rigaku D/Max-IIB) using a copper target and nickel filter. The surface and cross-section of coated powders were examined by scanning electron microscopy (SEM). The distribution of elements were analysed by X-ray dot mapping and elemental line scanning by wavelength dispersive spectrometry (SEM-WDS Jeol JSM-35). The thermal stability and weight change were determined by differential thermal analysis (DTA) and thermogravimetric analysis (TGA) (Setaram TAG24) at 1450 °C under 1 atm nitrogen for 0.5 h.

2.3. Hot pressing

Samples were hot pressed at 1800 °C in nitrogen in a graphite furnace (Fuji Dempa High Mylti 5000) for 1 h under a pressure of 24.5 MPa.

2.4. Microstructural analysis

The microstructural analysis of hot-pressed composites was similar to that conducted for CVD-TiC powders, except that the hot-pressed samples were additionally scanned from 113°–128° with a low scanning rate of $1° \, min^{-1}$ by X-ray diffraction for phase identification.

2.5. Density and mechanical properties

The density was measured by the water displacement technique.

Flexural strength was measured in a four-point bending test on a universal testing machine (Shimadzu AGS 500D) at a displacement rate of $0.5 \, mm \, min^{-1}$. The outer and inner spans were 30 and 10 mm, respectively. The nominal dimensions of the testing bars were 3 mm × 3 mm × 45 mm with 45° edge chamfers.

Hardness was determined by applying a microhardness indent (Vickers, H_V, Akashi AVK-A) at 50 kg for 15 s. Fracture toughness was measured and calculated following Evans and Charles' derivation [11] using the indentation technique. Fracture surfaces and crack propagation behaviour were scrutinized using optical microscopy and SEM.

3. Results and discussion

3.1. Analysis of TiN-coated TiC powders

The X-ray diffraction profiles of as-received TiC and CVD-TiC powder are both shown in Fig. 2. No trace of phases other than TiN and TiC could be detected in CVD-TiC powders. The scanning electron micrographs exhibited a uniform, grainy layer of TiN on the surfaces of TiC particles (Fig. 3) [9, 10]. Measurements of the cross-section of CVD-TiC particles indicated the thickness of the grainy layer was 1–2 μm.

3.2. Chemical interactions

A scanning electron micrograph of TiC/Si_3N_4 hot pressed at 1800 °C for 1 h in a nitrogen atmosphere is shown in Fig. 4a. TiC particles, with surrounding pores, became irregular and isolated islands after

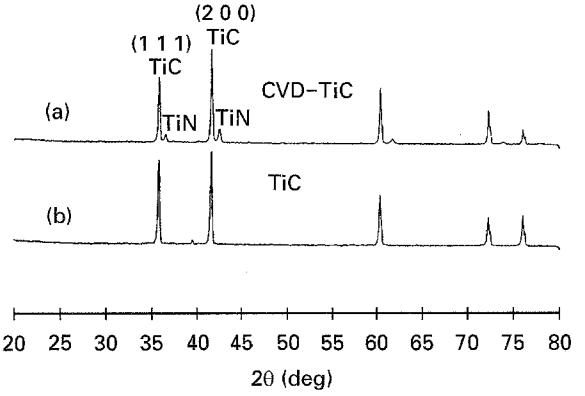

Figure 2 X-ray diffraction profiles of (a) TiN-coated TiC, and (b) as-received TiC.

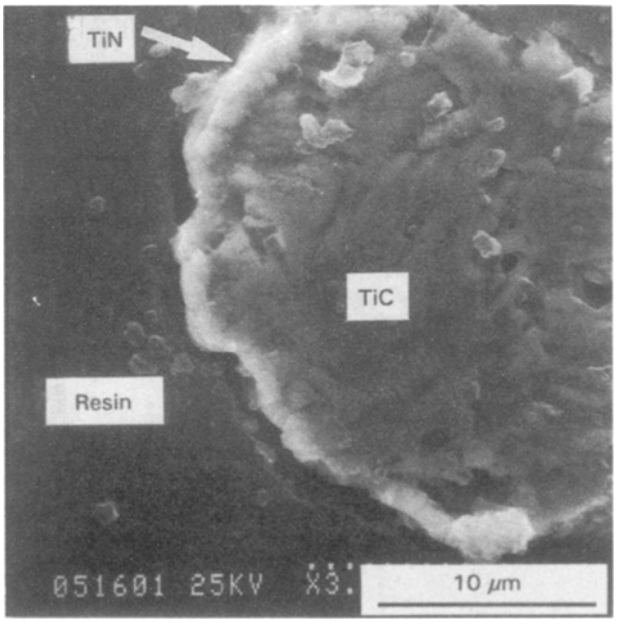

Figure 3 Scanning electron micrograph showing a cross-section of TiN-coated TiC.

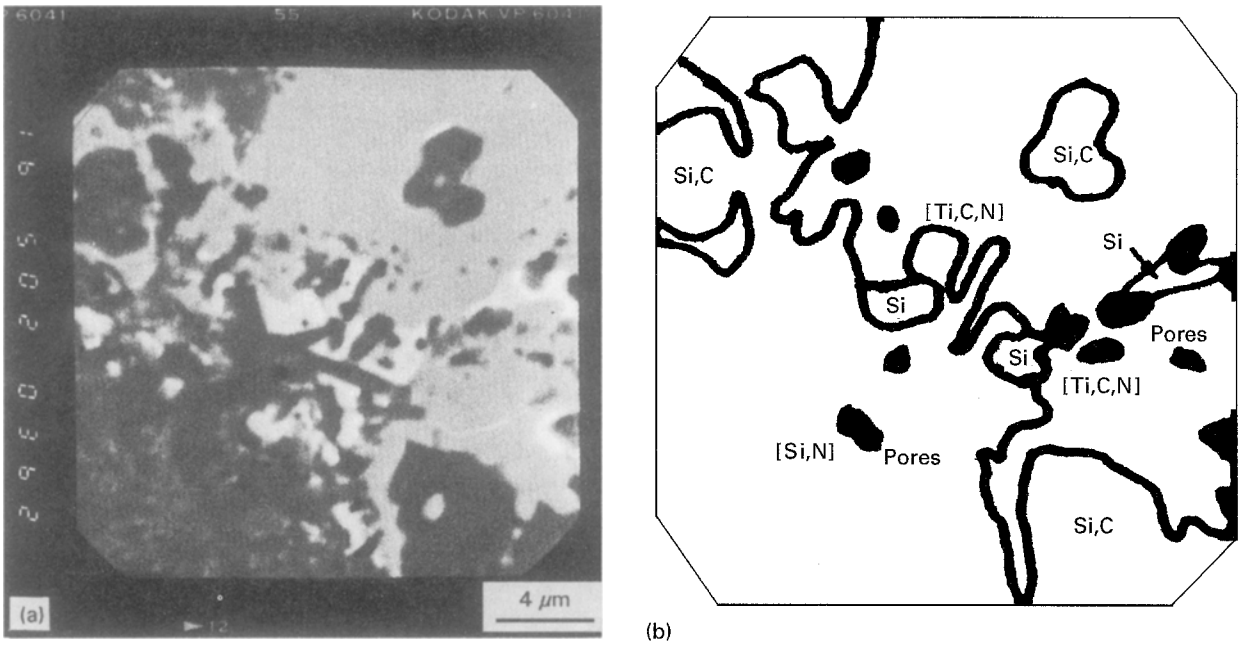

Figure 4 (a) A typical scanning electron micrograph of as-received TiC/Si_3N_4 composite, and (b) a schematic representation of (a). Samples were hot pressed at 1800 °C, 1 h, in a nitrogen atmosphere.

sintering. This was probably due to the chemical reactions which occurred between the Si_3N_4 matrix and TiC, associated with the evolution of nitrogen gas during hot pressing, as previously reported [5, 6].

A wavelength-dispersive spectrometer was used to analyse the distribution of elements carbon, nitrogen, titanium and silicon in Fig. 4a, and are shown in Fig. 4b. Reactants were found inside or between TiC particles and identified as β-Si_3N_4, a mixture of TiC, titanium carbonitride, SiC and a trace of iron silicide [6].

Low-angle X-ray analysis from 20°–80° with a scanning rate of 4° min^{-1} was unable to discern differences in phases between samples containing as-received TiC and CVD-TiC. They were therefore further analysed separately by XRD at a low scanning rate of 1° min^{-1} from 113°–128°. Results indicated that slightly larger amounts of titanium carbonitride solid solution and SiC phases were detected in CVD-TiC/Si_3N_4 samples than in TiC/Si_3N_4.

According to previous reports [7, 8], there was no noticeable chemical interaction between TiN and Si_3N_4 up to a temperature of 1800 °C. DTA/TGA analysis was therefore focused on TiN-coated TiC/Si_3N_4 samples to investigate the possible interactions between the TiN coating and TiC. Because it was formerly reported that TiC could react with nitrogen to form titanium nitride at temperatures above 1500 °C in a nitrogen atmosphere [12], a holding temperature of 1450 °C, 0.5 h, in 1 atm N_2 with a heating rate of 10 °C min^{-1} was selected for conducting the DTA/TGA analysis.

DTA results indicated that both heat absorption and exothermic peaks were observed at 1200 °C during the heating and cooling cycles for TiN-coated powders, which were not evident in as-received TiC. In addition, the TiN-coated TiC powders had an obvious weight loss of 1 mg during the holding

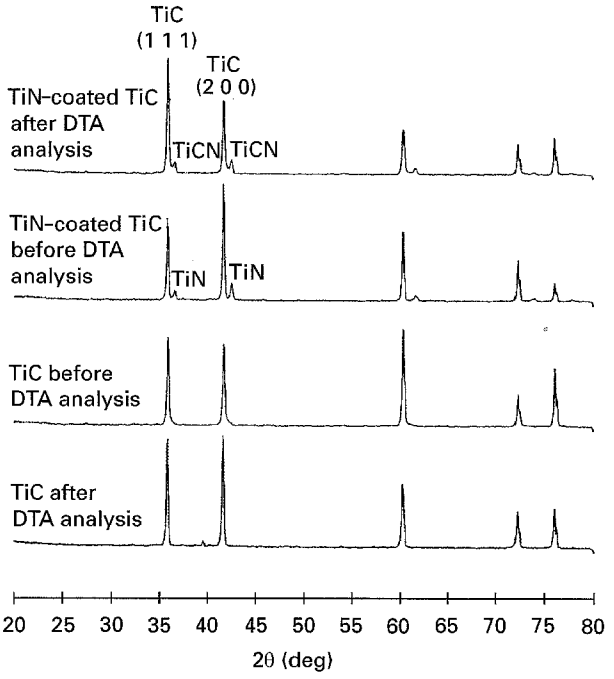

Figure 5 Results of X-ray diffraction profiles of TiC and TiN-coated TiC powders before and after DTA/TGA analysis.

period of 1450 °C but not in the as-received TiC powders.

Further examination by X-ray diffraction was conducted on both TiN-coated and as-received TiC powders after being tested by DTA/TGA at 1450 °C (Fig. 5). The preferred texture was progressively altered from (2 0 0) to (1 1 1) after heat treatment conducted during the DTA/TGA test. Additionally, after the DTA/TGA test at 1450 °C, TiN peaks had a tendency to move towards TiC to form a Ti(C,N) solid solution.

Using the same derivation as reported previously [6], and assuming the solid solution of titanium

carbonitride to be ideal, the composition of titanium carbonitride solid solution in Fig. 5 could be determined from the measured lattice parameter by X-ray diffraction profiles and Vegard's law [13, 14]. A composition of $TiC_{0.13}N_{0.87}$ was then obtained in TiN-coated TiC powders after being heat treated at 1450 °C, 0.5 h, in 1 atm N_2 atmosphere.

Polarized high-resolution optical microscopy was used to examine finely polished TiN-coated TiC/Si_3N_4 composite after being hot pressed at 1800 °C, 1 h. Observations revealed that the TiC particulates were uniformly coated by dense peripheral layers with a thickness of approximately 1.5 μm. Further examination by line scanning pointed out that the major elements in the layers were titanium, nitrogen and carbon (Fig. 6). Results suggested that the interfacial layers could probably be titanium carbonitride.

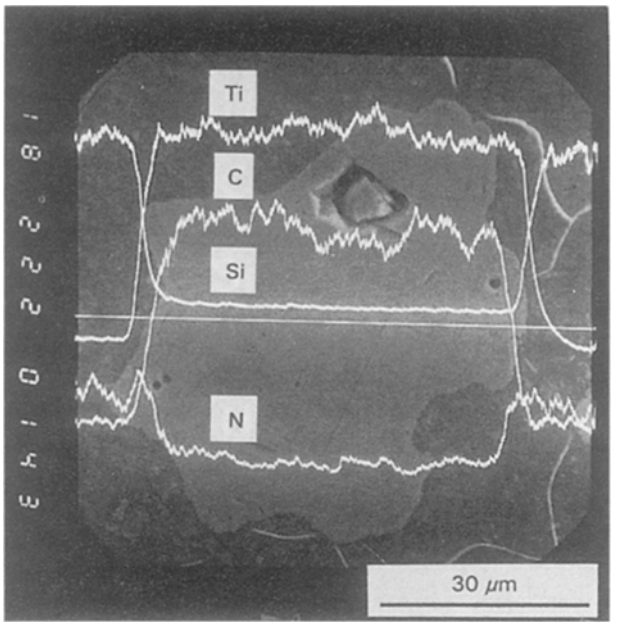

Figure 6 Line scanning of titanium, carbon, silicon and nitrogen elements along a line across the interfaces in a TiN-coated TiC/Si_3N_4 composite.

A scanning electron micrograph of CVD-TiC/Si_3N_4 composite hot-pressed at 1800 °C for 1 h in a nitrogen atmosphere is shown in Fig. 7a. A wavelength-dispersive spectrometer dot mapping was used to analyse the distribution of elements silicon, titanium, carbon and nitrogen. A sketch was then made (Fig. 7b) to express the overall distribution of elements in Fig. 7a, where three distinct areas are discernible. They were identified as TiC, Ti(C,N) and β-Si_3N_4 phases.

In as-received TiC/Si_3N_4 samples, the titanium carbonitride solid solution was formed by the reactions between silicon nitride and TiC particulates during hot pressing at 1800 °C [5, 6]. Nevertheless, in CVD-TiC/Si_3N_4 composites, the formation of titanium carbonitride solid solution started via the reactions between the TiC and TiN coating at 1450 °C, a temperature substantially lower than the dissociation temperature of silicon nitride [15]. A direct reaction between TiC and Si_3N_4 at elevated temperatures could therefore be avoided owing to the formation of titanium carbonitride.

3.3. Thermodynamic considerations

Pastor [14] investigated the thermodynamic stability of $TiC_{1-x}N_x$ and defined the domain of existence of $TiC_{1-x}N_x$ in a $(\ln P_{N_2})$–T–x diagram. Following the same derivations by Pastor, plots of $\ln P_{N_2}$ versus x at fixed temperatures of 1450 and 1800 °C could be drawn (Fig. 8a, b). These figures are very useful because, for a given concentration, x, and experimental nitrogen atmosphere, they allow us to predict the present phases. Fig. 8a and b shows marked boundaries of the four following domains: $TiC_{1-x}N_x$ plus titanium, pure $TiC_{1-x}N_x$, $TiC_{1-x}N_x$ plus carbon, and TiN plus carbon.

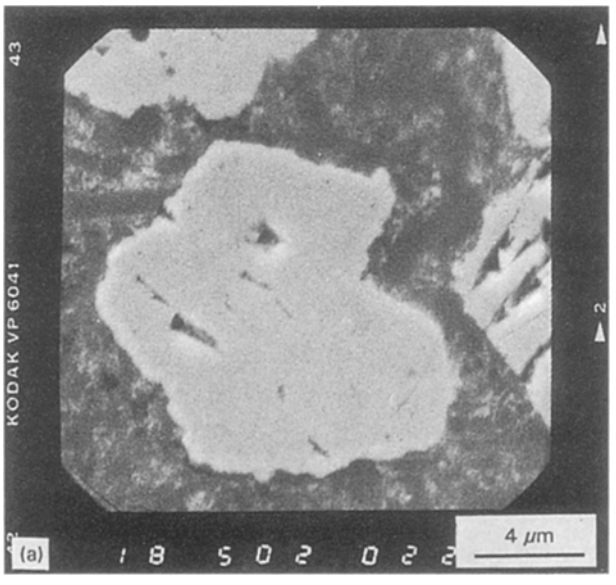

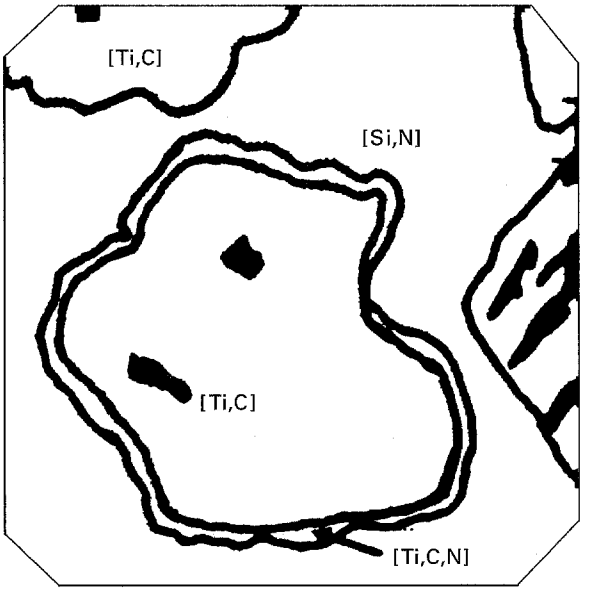

Figure 7 (a) A typical scanning electron micrograph of CVD-TiC/Si_3N_4 composite, and (b) a schematic representation of (a). Samples were hot pressed at 1800 °C, 1 h, in a nitrogen atmosphere.

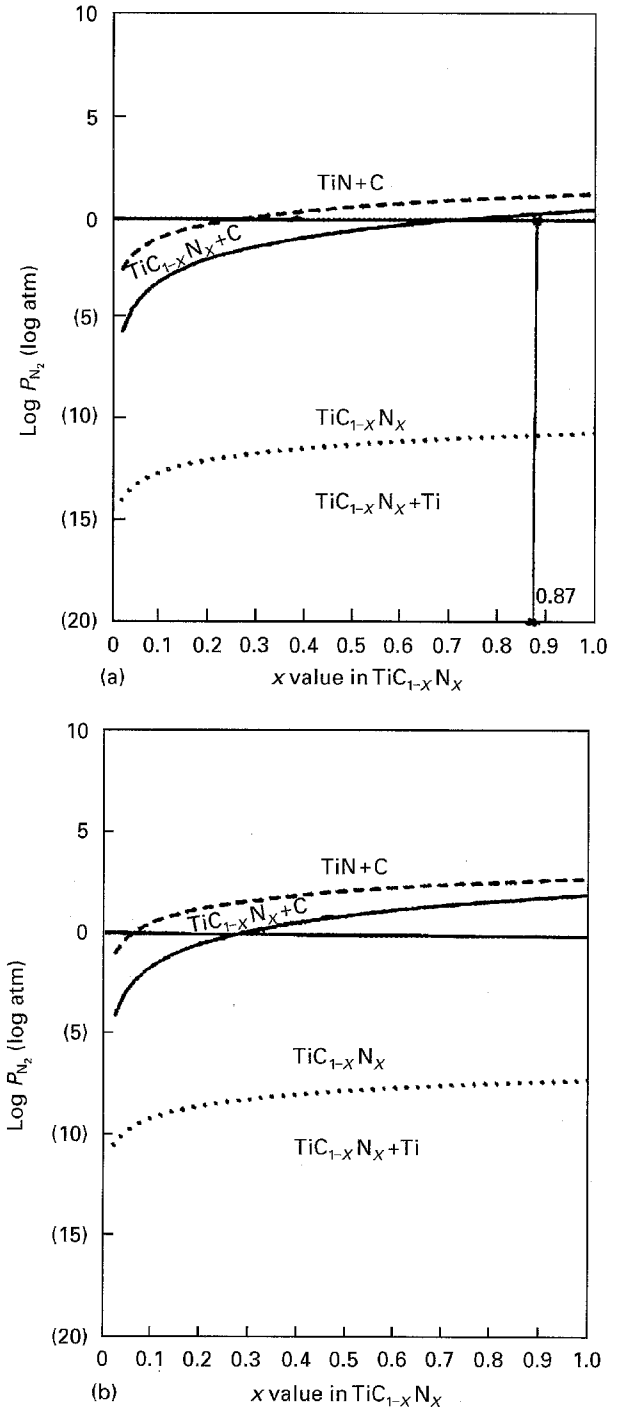

Figure 8 The equivalent partial pressure of nitrogen gas versus the composition, x, in $Ti_{1-x}N_x$ at (a) 1450 °C, and (b) 1800 °C.

A point corresponding to the experimental conditions of 1 atm N_2 pressure, 1450 °C, and a composition of $TiC_{0.13}N_{0.87}$, was slightly below the boundary line and within a region where the $TiC_{1-x}N_x$ was stable (Fig. 8a). This is consistent with the observation of titanium carbonitride solid solution from X-ray diffraction results (Fig. 5).

The boundary lines in Fig. 8a moved upwards as the temperature was increased to 1800 °C (Fig. 8b), indicating that a region with the coexistence of titanium carbonitride and carbon was passed through, with increasing temperature for TiN-coated TiC/Si_3N_4 samples sintered at 1 atm N_2 pressure. This was probably why the SiC phase was observed in samples sintered at 1800 °C.

Based on the microstructural analysis and X-ray diffraction results, the reactions in TiN-coated TiC/Si_3N_4 and as-received TiC/Si_3N_4 could, respectively, be expressed by the following equations [6, 14].

In TiN-coated TiC/Si_3N_4

$$(1-x)\,TiC + x\,TiN = TiC_{1-x}N_x \quad (1)$$

$$TiC_{1-x}N_x + (x'-x)/2\ N_2 = TiC_{1-x'}N_{x'} + (x'-x)C \quad (x' \geqslant x) \quad (2)$$

In as-received TiC/Si_3N_4

$$TiC + x/2\,N_2 = TiC_{1-x}N_x + xC \quad (3)$$

By substituting $T = 1450$ °C and $x = 0.87$ into Equation 1, $\Delta G^\circ_{1450} = -42\,567$ cal mol^{-1} can be obtained, which is much more negative than the change of standard Gibbs' energy in Equation 3. This indicates that the formation of titanium carbonitride solid solution was thermodynamically possible in TiN-coated TiC/Si_3N_4 at 1450 °C, but not as evident in as-received TiC/Si_3N_4. This is quite similar to what was observed in X-ray diffraction analysis (Fig. 5).

Because the formation of titanium carbonitride in CVD-TiC/Si_3N_4 occurred at 1450 °C, which was much lower than the decomposition temperature of Si_3N_4, the nitrogen source for Equation 2 was very likely from the nitrogen atmosphere. In addition, the formation of $TiC_{1-x}N_x$ could inhibit further interactions between the TiC particles and the Si_3N_4 matrix at elevated temperatures.

3.4. Physical and mechanical properties

3.4.1. Density

The measured bulk density of TiC/Si_3N_4 composite increased with TiC contents because the theoretical density of TiC ($\rho = 4.93$ g cm^{-3}) is substantially greater than that of monolithic Si_3N_4 ($\rho = 3.256$ g cm^{-3}). Because the theoretical density of the composite was difficult to determine, owing to the uncertain density of interfacial phases, the open porosity was measured as an indication of densification. The open porosities of samples containing up to 30 vol % as-received and CVD-coated TiC, hot pressed at 1800 °C, 1 h, in 1 atm N_2 atmosphere, are shown in Fig. 9. The open porosities of both composites were found to increase as the TiC content increased. Additionally, the composites containing CVD-coated TiC had considerably less pore volume than that of samples containing as-received TiC. The differences in porosity became greater with increasing TiC contents.

Optical micrographs of polished surface revealed interfacial pores near the interfaces in a CVD-TiC/Si_3N_4 composite, but pores were not obvious in TiN-coated/Si_3N_4. This strongly suggests that the TiN coating played an extremely essential role in diminishing the reactions between the TiC and Si_3N_4, and thus reduced pores and enhanced the densification.

3.4.2. Hardness and flexural strength

The hardness of CVD-TiC/Si_3N_4 and as-received TiC/Si_3N_4 composites versus TiC content are shown

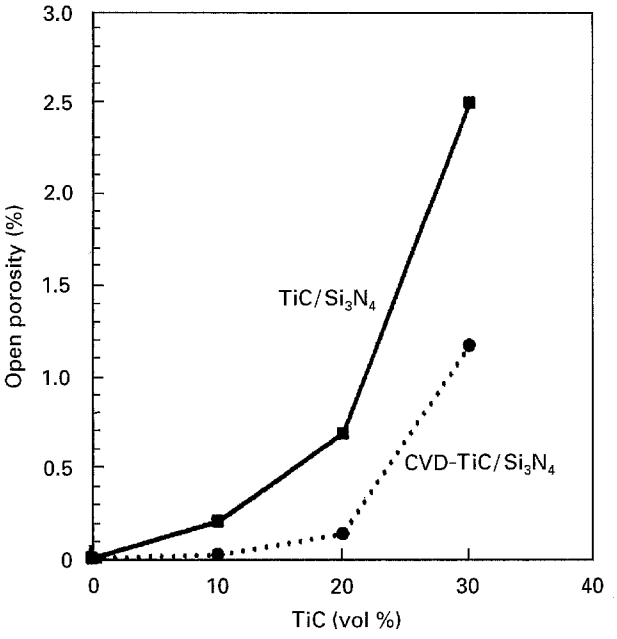

Figure 9 Open porosity of as-received TiC/Si_3N_4 and CVD-TiC/Si_3N_4 composites versus TiC content. Samples were hot pressed at 1800 °C for 1 h, in 1 atm N_2.

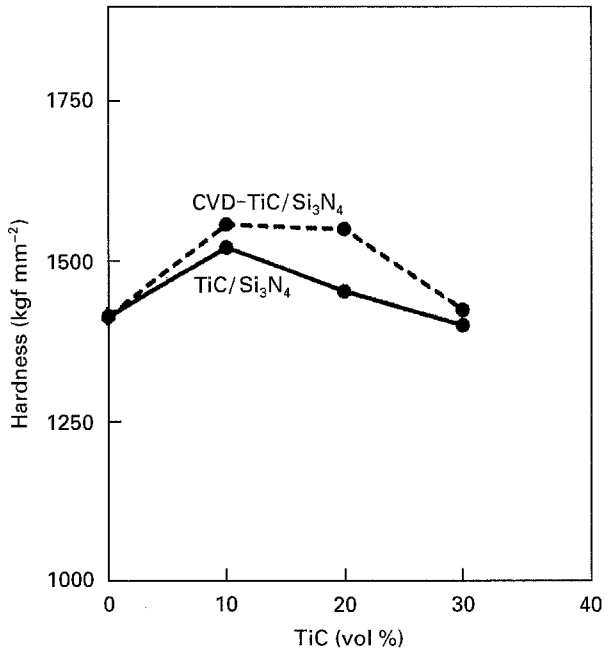

Figure 10 Hardness of CVD-TiC/Si_3N_4 and as-received TiC/Si_3N_4 composites versus TiC content. Samples were hot pressed at 1800 °C for 1 h in 1 atm N_2.

in Fig. 10. The hardness of CVD-TiC/Si_3N_4 was consistently greater than that of as-received TiC/Si_3N_4 composites, and reached a maximum value at 20% TiC.

The four-point bending strengths of CVD-TiC/Si_3N_4 and as-received TiC/Si_3N_4 composites versus TiC content are plotted in Fig. 11. Results indicated the strength decreased with increasing TiC content. The physical mismatch and chemical reactions between TiC and Si_3N_4 probably caused a decrease in hardness and strength in samples with high TiC content. The degradation was particularly phenomenal in

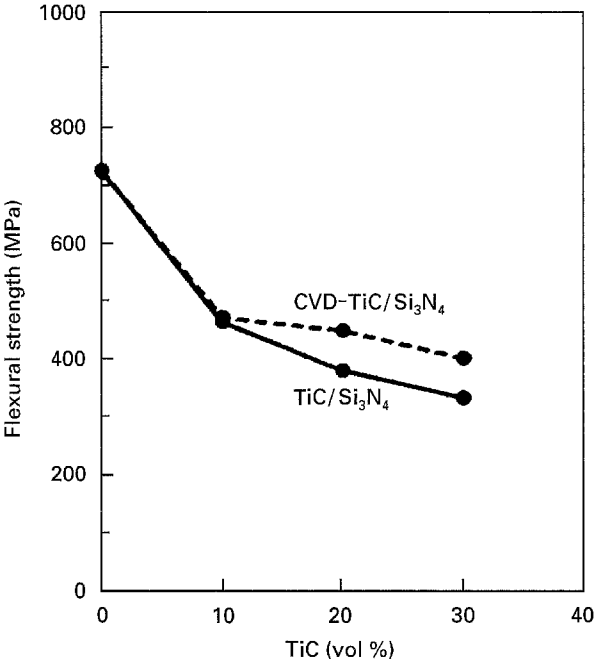

Figure 11 Flexural strength of CVD-TiC/Si_3N_4 and as-received TiC/Si_3N_4 composites versus TiC content. Samples were hot pressed at 1800 °C for 1 h in 1 atm N_2.

composites containing uncoated TiC.

Following Evans and Faber's analysis [16], a critical particle size for spontaneous microcracking to occur in TiC/Si_3N_4 composites was calculated as 17 μm. Some TiC particles up to this size were observed from scanning electron micrographs. The spontaneous microcracking induced by large TiC particles could be one factor responsible for the decrease in strength with the addition of TiC.

3.4.3. Fracture toughness and toughening mechanisms

Fracture toughness measured by the surface indentation technique [11] for composites containing various compositions of as-received and CVD-TiC are shown in Fig. 12. A maximum toughness value of 6.9 MPa $m^{1/2}$, approximately 25% higher than that of monolithic Si_3N_4 processed under the same experimental conditions, was obtained in 20 vol % CVD-TiC/Si_3N_4 samples. A tendency of decreasing toughness was observed in composites with 30% TiC. This was probably due to the inhibition of β-Si_3N_4 grain growth and difficulties in dispersion as the TiC content increased [17]. The fracture toughness of composites with CVD-TiC was invariably greater than that of samples with as-received TiC. This was possibly because the TiN coating efficiently reduced the reactions between TiC and Si_3N_4 and reduced interfacial pores.

Examination of as-received TiC/Si_3N_4 by scanning electron microscopy clearly illustrated that cracks propagated into TiC particles, and were deviated along preferred orientations with large angles [17]. Some branching and microcrackings were also observed inside TiC.

The crack propagating behaviour in CVD-TiC/Si_3N_4 composites was quite different, however.

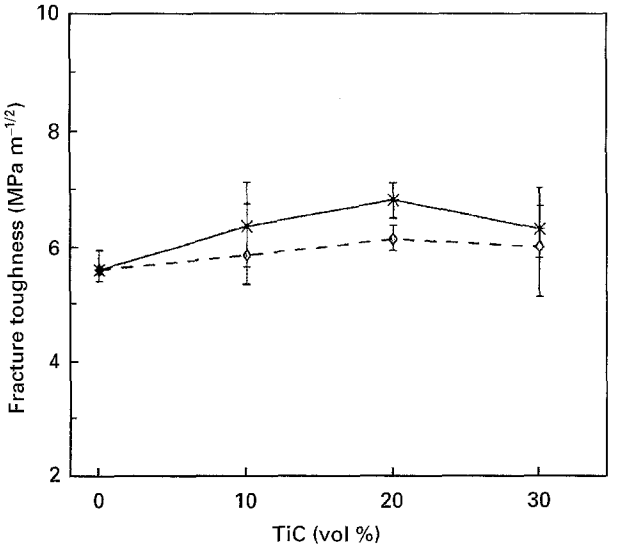

Figure 12 Fracture toughness of (◇) as-received TiC/Si_3N_4 and (✳) CVD-TiC/Si_3N_4 composites versus TiC content. Samples were hot pressed at 1800 °C for 1 h in 1 atm N_2.

The cracks did not pass into TiC particles, but propagated along the interfaces between TiC and Si_3N_4 instead. The differences in thermal expansion coefficients (TCE) and elastic modulus between Si_3N_4, TiC and TiN, caused compressive hoop stress and tensile radial stress near the interfaces. This is particularly phenomenal in composites containing TiN-coated TiC, because the TiN had an exceptionally large value of TCE ($\alpha_{TiN} = 9.4 \times 10^{-6}\,°C^{-1}$). The residual stress could therefore deflect an approaching crack and enhance fracture toughness [8, 17, 18].

The interfacial bonding between TiC and Si_3N_4 appeared reasonably good from the examination of scanning electron micrographs and the observation of secondary fracture with typical brittle patterns of mirror and hackle in the TiC particles [17]. That load transfer from the matrix to a higher Young's modulus dispersoid could be an effective toughening mechanism in ceramic matrix composites was previously reported [19, 20]. The Young's modulus of TiC ($E = 429$ GPa) is considerably higher than that of Si_3N_4 ($E = 304$ GPa). The load-transfer mechanism could, therefore, also play a role in the toughening effects.

The thermal mismatch between TiC and Si_3N_4 could generate periodic residual tension in the TiC particles and residual compression in the matrix in the composites. Estimated values of increased toughness due to the periodic residual stress were calculated following Taya *et al.* and Cutter and Virkar's analyses [21, 22]. The calculated values were greater than the measured toughness, however.

In brief, the toughening mechanisms in TiC/Si_3N_4 and TiN-coated TiC/Si_3N_4 composites would be attributed to crack deflection, load transfer and crack impedence by the periodic compressive residual stress. A more uniform TiN coating, through a better coating technique, would definitely improve the toughness.

4. Conclusions

1. A TiN layer has been successfully coated on the TiC powders by the CVD method. The formation of titanium carbonitride solid solution ($TiC_{0.13}N_{0.87}$) occurred at 1450 °C by the reaction of TiN and TiC in a TiN-coated TiC/Si_3N_4 composite, which effectively reduced the subsequent interactions between TiC and Si_3N_4 and enhanced the densification.

2. The observation of SiC phase was explained from plots of nitrogen partial pressure versus composition, x, at fixed temperatures. The mechanisms of the formation of titanium carbonitride in CVD-TiC/Si_3N_4 and as-received TiC/Si_3N_4 were proposed based on thermodynamic calculations and phase analysis.

3. TiN-coated TiC/Si_3N_4 composites exhibited less pore volume, greater hardness, flexural strength and toughness than those of as-received TiC/Si_3N_4 samples.

4. Cracks propagated into TiC particles, and deviated along preferred orientations with large angles in as-received TiC/Si_3N_4 samples, whereas in TiN-coated TiC/Si_3N_4 composites, cracks propagated along the interfaces between the TiC and Si_3N_4 matrix.

5. The toughening mechanisms in TiC/Si_3N_4 and TiN-coated TiC/Si_3N_4 composites have been attributed to crack deflection, load transfer and crack impedence by compressive thermal residual stress.

Acknowledgement

The authors thank the National Science Council, Taiwan, for support under grant NSC 83-0404-D006-001.

References

1. T. I. MAH, M. G. MENDIRATTA and H. A. LIPSITT, *Am. Ceram. Bull. Soc.* **60** (1981) 1229.
2. C. MARTIN, B. CALES, P. VIVIER and P. MATHIEU, *Mater. Sci. Eng.* **A109** (1989) 351.
3. G. ZILBERSTEIN and S. T. BULJAN, *Adv. Mater. Charact. II. Mater. Sci. Res.* **19** (1985) 389.
4. B. SARUHAN and G. ZIEGLER, in "Advanced Structural Inorganic Composites", edited by P. Vincenzini (Elsevier Science, New York, 1991) pp. 563–71.
5. S. T. BULJAN and G. ZILBERSTEIN, *Mater. Sci. Res.* **20** (1986) 305.
6. J. L. HUANG, H. L. CHIU and M. T. LEE, *J. Am. Ceram. Soc.* **77** (1994) 705.
7. A. SMITH, A. ABED, H. J. EDREES and A. HENDRY, "Ceramic Matrix Composites of Silicon Nitride with Conducting Particles", Key Engineering Materials, Vol. 89–91 (Trans Tech, Switzerland, 1994) pp. 423–8.
8. J. L. HUANG, S. Y. CHEN and M. T. LEE, *J. Mater. Res.* **9** (1994) 2349.
9. H. ITOH, K. HATTORI and S. NAKA, *J. Mater. Sci.* **24** (1989) 3643.
10. K. TSUGEKI, T. KATO, Y. KOYANAGI, K. KUSAKABE and S. MOROOKA, *J. Mater. Sci.* **28** (1993) 3168.
11. A. G. EVANS and E. A. CHARLES, *J. Am. Ceram. Soc.* **59** (1976) 371.
12. Y. YASUTOMI, M. DOBUE, S. SHINOZAKI and J. HANGAS, *J. Ceram. Soc. Jpn. Int. Edn.* **99** (1991) 676.
13. B. D. CULLITY, "Elements of X-ray Diffraction", 2nd Edn (Addison–Wesley, Massachusetts, 1978) p. 376.

14. H. PASTOR, *Mater. Sci. Eng.* **A105/106** (1988) 401.
15. S. N. LAKIZA, *Thermochim. Acta.* **93** (1985) 577.
16. A. G. EVANS and K. T. FABER, *J. Am. Ceram. Soc.* **64** (1981) 394.
17. H. L. CHIU and J. L. HUANG, *Ceram. Int.* **20** (1994) 49.
18. G. C. WEI and P. F. BECHER, *ibid.* **67** (1984) 571.
19. R. W. RICE, *Ceram. Eng. Sci. Proc.* **2** (1981) 661.
20. C. J. LIN and J. L. HUANG, *J. Mater. Sci.* **28** (1993) 1074.
21. M. TAYA, S. HAYASHI, A. S. KOBAYASHI and H. S. YOON, *J. Am. Ceram. Soc.* **73** (1990) 1382.
22. R. A. CUTLER and A. V. VIRKAR, *J. Mater. Sci.* **20** (1985) 3557.

Received 1 December 1994
and accepted 13 February 1996